

# Enhanced delivery of AAV-like nanoparticles after blood-brain barrier disruption in a mouse model

Josquin Foiret  
Department of Radiology  
Stanford University  
Palo Alto, CA, USA  
jlfoiret@stanford.edu

Jai Woong Seo  
Department of Radiology  
Stanford University  
Palo Alto, CA, USA  
jaiwseo@stanford.edu

Hua Zhang  
Department of Radiology  
Stanford University  
Palo Alto, CA, USA  
hchzhang@stanford.edu

Hamilton Kakwere  
Department of Radiology  
Stanford University  
Palo Alto, CA, USA  
hkakwere@stanford.edu

Lisa M. Mahakian  
Department of Biomedical Engineering  
UC Davis  
Davis, CA, USA  
lmahakian@ucdavis.edu

Sarah Tam  
Department of Biomedical Engineering  
UC Davis  
Davis, CA, USA  
smjohns@ucdavis.edu

Katherine W. Ferrara  
Department of Radiology  
Stanford University  
Palo Alto, CA, USA  
kwferrara@stanford.edu

**Abstract**— Focused ultrasound (FUS) to open the blood brain barrier (BBB) is under evaluation for the delivery of therapeutic agents to the brain. Regarding delivery of genes through the BBB, adeno-associated viruses (AAVs) have generated interest due to their ability to specifically and efficiently transfect the brain, which was recently demonstrated in mouse models. In this work, we investigated the use of 1.5 MHz FUS-mediated BBB opening in a mouse model after systemic injection of AAV-like polymer nanoparticles designed to have a 20-nm size and a targeting peptide similar to AAV-PHP.eB. Radiolabeling of the nanoparticles allowed *in vivo* tracking of the accumulation in the brain following the FUS treatment with positron emission tomography imaging (PET). Significant accumulation was measured in the treated hemisphere with a 1.8-fold enhancement compared to the contra-lateral hemisphere. Our experimental setup optimized for rodents (Verasonics) enables ultrasound imaging, precise targeting with electronic steering, and monitoring of the cavitation activity during the FUS treatment using passive acoustic mapping.

**Keywords**—focused ultrasound, passive acoustic mapping, blood brain barrier opening, nanoparticle, positron emission tomography.

## I. INTRODUCTION

Engineered adeno-associated viruses (AAV) are of interest to transfect the brain following systemic injection. AAVs with engineered capsids cross the blood brain barrier (BBB) and have been demonstrated to achieve high transfection in mouse models [1]. Recently, AAV-PHP.eB was shown to yield high transduction efficiency in the brain and spinal cord [2]. Combined with therapeutic genes, engineered AAV are a promising tool for treating diseases affecting the CNS but the pharmacokinetics (PK) of AAVs is still under investigation.

Blood brain barrier (BBB) disruption to deliver therapeutic agents through a combination of focused ultrasound (FUS) and microbubbles (MBs) is under evaluation for the treatment of brain cancer [3], [4]. In this study, we sought to investigate the PK of polymer nanoparticles (NPs) mimicking the peptide

introduced for enhanced accumulation and the size (20 nm) of AAV-PHP.eB following FUS-mediated BBB disruption. With our experimental setup optimized for rodents, electronic steering of the therapeutic beam was employed to offer a treatment of 24 (axial)  $\times$  18 (transverse)  $\times$  16 (transverse) mm<sup>3</sup> without generating significant grating lobes [5]. After MB injection, electronic sweeping of the narrow beam within the brain can offer precise delimitation of the larger sonicated area.

NPs were radiolabeled for *in vivo* tracking in the mouse brain with positron emission tomography (PET) imaging. Recent studies have shown that the location and concentration of radiolabeled gold nanoclusters (size: 5.6 nm) could be predicted by passive acoustic mapping [6]. Delivery of larger molecules such as AAV requires stronger disruption of the BBB [7] and in this work we quantified the differences in terms of accumulation of the AAV-like nanoparticle up to 21 hours after BBB disruption.

## II. METHODS

### A. Experimental protocol

Following approval by the Institutional Committee on Animal Use and Care, experiments were performed in 16 C57BL/6 mice (Charles River). The timeline of the protocol is summarized in Fig. 1. BBB disruption was induced using 1.5 MHz FUS and MBs in the right cortex after intravenous

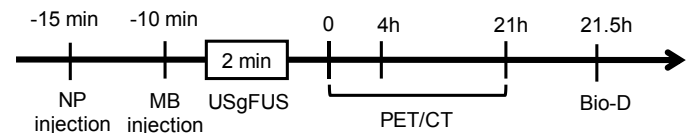


Fig. 1. Timeline of the experimental protocol. AAV-like radiolabeled nanoparticles (NPs) were injected just prior to FUS-mediated BBB disruption. Positron emission tomography (PET) was employed to track and quantify accumulation in the sonicated area up to 21h after the sonications. Final quantification was obtained with biodistribution.

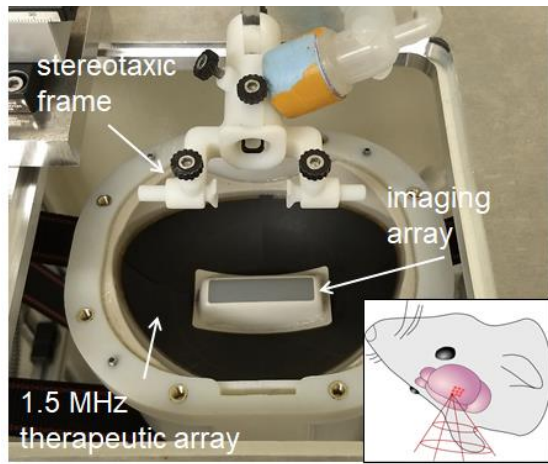


Fig. 2. Experimental setup. A 1.5 MHz 128-element therapeutic array was used to insonify the animals. Targeting and passive acoustic mapping was performed with a linear array located at the center of the therapeutic array (L12-5, Phillips/ATL). A 3D printed stereotaxic frame and was attached to a 3D stage for precise positioning and targeting. Ultrasound sonications were applied with the animal in the supine position as indicated in the lower right corner.

injection of the radiolabeled NPs. Following the ultrasound treatment, PET/CT imaging was performed at 0, 4 and 21 h to quantify accumulation in the treated and contra-lateral hemispheres. Animals were sacrificed for biodistribution and autoradiography after the 21 h time point. We divided the animals into 4 groups: NPs only (N=3), NPs+FUS (N=3), NPs+MBs (N=4), NPs+FUS+MBs (N=6).

**B. <sup>64</sup>Cu-labeled polymer nanoparticles**

The polymer NPs used in this study were engineered to mimic the size (20 nm) and the surface peptide of the AAV-PHP.eB targeting the brain endothelium [2]. The NPs were radiolabeled with copper-64 (half-life: 12.7 h) and isolated with size-exclusion chromatography. NPs (0.19±0.057 mg/mouse and 0.19± 0.072 mCi/mouse) were systemically-injected through the tail vein of the animals just prior to BBB disruption.

**C. FUS treatment**

A programmable ultrasound system (Vantage 256, Verasonics, Kirkland, VA, USA) was used to perform USgFUS treatment with real-time guidance and monitoring. The FUS treatment was done with a 1.5-MHz 128-element array allowing electronic steering (Imasonic, Voray sur l’Ognon, France) with a focal depth of 55 mm and a -6 dB focal dimension of 2.7 mm (axial) × 0.7 mm (transverse) × 0.4 mm (transverse). A full description of the array is given in [5]. The FUS treatment was realized by rapidly sweeping the focus along a square grid of 7x7 positions with steps of 0.5 mm (effective insonified volume ~3.5x3.5x2.7 mm<sup>3</sup> = 33 mm<sup>3</sup>) with each spatial position receiving a 1 ms burst (i.e. 49 ms to cover the entire grid). The grid repetition rate was set to 5 Hz and the total sonication time to 2 min. The peak negative pressure was set to 600 kPa as measured in water with a calibrated needle hydrophone (HNP0400, Onda, Sunnyvale, CA, USA). US imaging was done by an L12-5 (38 mm aperture, Phillips/ATL) positioned in the central opening of the FUS array. The same array was used for passive acoustic mapping during sonications. The L12-5 38 mm

has 192 elements and the central 128 elements were utilized here.

The animal was placed in the supine position with the head held by a stereotaxic frame designed in-house. We sought to target the cortex in the right hemisphere based on anatomical features with B-mode imaging. FUS sonications started 10 s after injecting a 50 µL bolus of 1.5×10<sup>7</sup> microbubbles in the tail vein of the animal. MBs were non-targeted and lipid shelled, produced in-house with a size range of 1-3 µm (median size: 1.6 µm). During treatment, anesthesia was maintained using isoflurane and pure O<sub>2</sub>.

**D. Passive acoustic mapping**

For the 7 spatial positions aligned with the imaging plane, RF signals were passively recorded during the FUS sonications with the imaging transducer. Real-time processing was implemented to display passive acoustic maps following the angular spectrum approach (ASPAM) [8]. Briefly, the signal recorded passively with the imaging array is backpropagated in the frequency domain to localize acoustic sources and conveniently allows detection in selected frequency bandwidths. We processed the PAM in three different bandwidths: harmonics, ultra-harmonics and broadband. The 4<sup>th</sup> to 8<sup>th</sup> harmonics (i.e. 6, 7.5, 9 and 10.5 MHz) were utilized to reconstruct the passive acoustic maps with a window bandwidth of 0.2 MHz and assumed to correspond to stable cavitation. Similarly, the 4<sup>th</sup> to 8<sup>th</sup> ultra-harmonics (i.e. 6.75, 8.25, 9.75 and 11.25 MHz) were considered in the analysis. The position of the maximum for each PAM map for each sonication was compared to the set position of the focal beam. All processing was implemented in Matlab (r2017a,

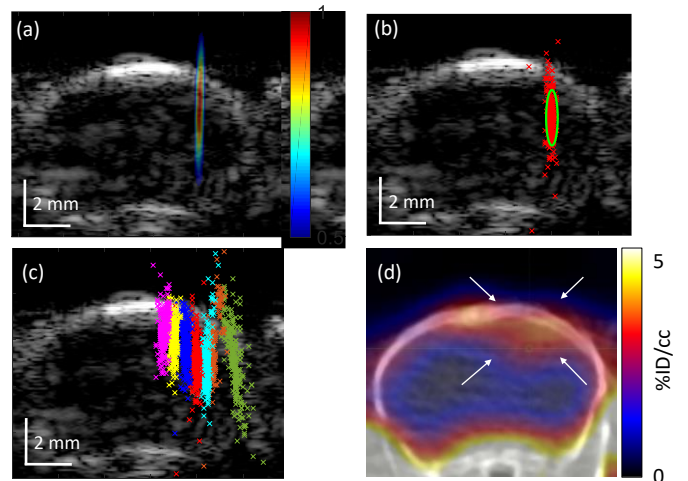


Fig. 3. Localizations of cavitation events with passive acoustic mapping coincide with increase radioactivity in the treated hemisphere indicating accumulation of nanoparticles. (a) Passive acoustic map (color) calculated using the angular spectrum method for a single sonication for one spatial position of the grid. The map was processed using the 4<sup>th</sup> to 8<sup>th</sup> harmonics of the 1.5 MHz therapeutic transmission. The background is the B-mode image outlining the skull. (b) At a given spatial position of the grid, the positions of the maximum for each of the 600 sonications (120 s of recording at 5 Hz PRF) depicts a precise region for cavitation. For reference, the set location for the therapeutic focus (electronic steering) is indicated by the green line (FWHM). (c) Summary of all cavitation localizations for the 7 spatial locations aligned with the imaging plane. (d) PET/CT scan at 4 h after the FUS treatment indicates increased activity in the sonicated area.

Mathworks, Natick, MA, USA) to work in real-time within the Verasonics Matlab-based software interface.

### E. Quantification of nanoparticles accumulation

Statistical analysis was performed on the PET data by region of interest (ROI) analysis in the targeted hemisphere and in the contra-lateral hemisphere. Quantifications were also calculated between the two hemispheres with the biodistribution data.

## III. RESULTS

### A. Localization of cavitation

A typical ASPAM map in the presence of circulating MBs is shown in Fig. 3(a). Localizing the maximum of each map over the 120 s of sonication yielded precise delineation of the cavitation region and was in agreement with the beam focal positions set with electronic steering (Fig. 3(b)). Combining all of the localizations obtained for the 7 recorded positions (Fig. 3(c)) depicted clear separation between individual spatial locations of the grid pattern (spaced by 0.5 mm). An interesting finding was that although the grid of focal positions was planar, the cavitation localizations showed a clear curvature following the skull geometry. Some spatial locations close to the skull were found to show cavitation slightly away from the set location of the beam which could originate from the presence of a larger vessel near the skull. It should be noted that no ultraharmonics were detected during the treatments suggesting a stable cavitation regime for the parameters used in this study. The precise targeting of the right cortex was also evidenced by PET imaging where local accumulations higher than 3 % injected dose/cc were measured in the treated hemispheres as depicted in Fig. 3(d).

### B. Nanoparticles pharmacokinetics

PK analysis of the PET data showed significant uptake in the FUS-treated hemisphere at 0, 4 and 21 h (Fig. 4(a)). From the bio-distribution, the NP accumulation was found to be enhanced by 1.8-fold in the entire FUS-treated hemisphere with respect to the contra-lateral hemisphere (Fig. 4(b)). No difference was seen in the MB-only group (Fig. 4(c)) while a slight but significant decrease was witnessed in the treated hemisphere of the FUS only group.

## IV. CONCLUSION AND DISCUSSION

In this study, we investigated the accumulation of polymer NPs after FUS-mediated BBB disruption by mimicking the targeting peptide and size of AAV-PHP.eB. To our knowledge, *in vivo* tracking of such NPs using radiolabeling has only been sparsely studied [6], [9]–[11] and is of great interest considering their 20 nm size.

Our 1.5 MHz FUS experimental setup designed for rodents offers accurate targeting for localized BBB opening. Combined with the Verasonics platform, the FUS treatment can be monitored in real time using passive acoustic mapping. To expand the treated volume, we insonified the mouse brain by electronically sweeping the FUS beam and found that we could clearly separate cavitation events spaced by 0.5 mm.

Using PET/CT imaging, we measured a significant increase in radioactivity in the treated hemisphere indicating

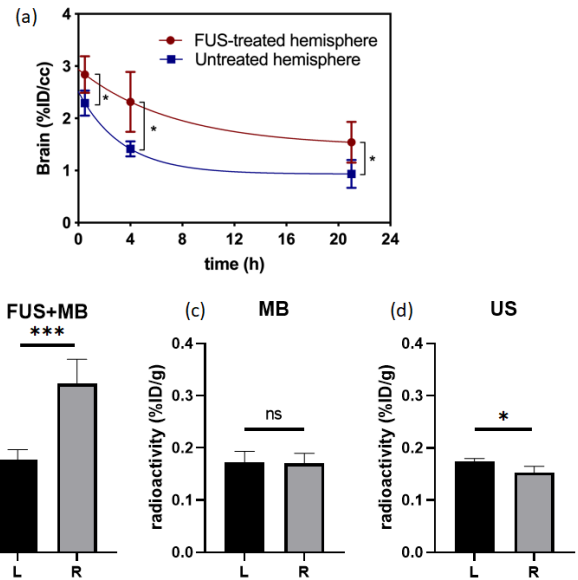


Fig. 4. Pharmacokinetics and biodistribution showed increased accumulation in the FUS treated hemisphere. (a) Time activity curve from the PET images in the FUS-treated versus the contralateral hemisphere (ROI analysis) depicting higher significant uptake in the FUS-treated brain region. (b-d) Biodistribution analysis at 21.5 h after the administration of NP. (b) Biodistribution showed a significant increase in radioactivity (1.8-fold) in the MBs+FUS-treated hemisphere. (c) No difference between hemispheres were seen in the group receiving MBs only. (d) A reduction in radioactivity in the treated hemisphere was measured in the FUS only group. L: left, R: right. Statistical significance: \*\*\* $p < 0.001$ , \* $p < 0.05$ .

accumulation of NPs. This result was supported by biodistribution showing a 1.8-fold enhancement in the treated hemisphere.

### ACKNOWLEDGMENT

This work was supported by NIH grants R01CA112356, R01CA227687, R01EB026094 and R01 EB028646.

### REFERENCES

- [1] B. E. Deverman *et al.*, “Cre-dependent selection yields AAV variants for widespread gene transfer to the adult brain,” *Nat. Biotechnol.*, 2016.
- [2] K. Y. Chan *et al.*, “Engineered AAVs for efficient noninvasive gene delivery to the central and peripheral nervous systems,” *Nat. Neurosci.*, 2017.
- [3] “ExAblate (Magnetic Resonance-guided Focused Ultrasound Surgery) Treatment of Brain Tumors.” [Online]. Available: <https://clinicaltrials.gov/ct2/show/NCT01473485>.
- [4] “MRI-Guided Focused Ultrasound Feasibility Study for Brain Tumors.” [Online]. Available: <https://clinicaltrials.gov/ct2/show/NCT00147056>.
- [5] J. Liu, J. Foiret, D. N. Stephens, O. Le Baron, and K. W. Ferrara, “Development of a spherically focused phased array transducer for ultrasonic image-guided hyperthermia,” *Phys. Med. Biol.*, 2016.
- [6] Y. Yang *et al.*, “Cavitation dose painting for focused ultrasound-induced blood-brain barrier disruption,” *Sci. Rep.*, 2019.
- [7] H. Chen and E. E. Konofagou, “The size of blood-brain barrier opening induced by focused ultrasound is dictated by the acoustic pressure,” *J. Cereb. Blood Flow Metab.*, 2014.
- [8] C. D. Arvanitis, C. Crake, N. McDannold, and G. T. Clement, “Passive Acoustic Mapping with the Angular Spectrum Method,” *IEEE Trans. Med. Imaging*, 2017.

- [9] K. J. Lin *et al.*, "Quantitative micro-SPECT/CT for detecting focused ultrasound-induced blood-brain barrier opening in the rat," *Nucl. Med. Biol.*, 2009.
- [10] F. Y. Yang *et al.*, "Pharmacokinetic Analysis of <sup>111</sup>In-Labeled Liposomal Doxorubicin in Murine Glioblastoma after Blood-Brain Barrier Disruption by Focused Ultrasound," *PLoS One*, 2012.
- [11] H. Kim, M. A. Park, S. Wang, A. Chiu, K. Fischer, and S. S. Yoo, "PET/CT imaging evidence of FUS-mediated (18)F-FDG uptake changes in rat brain," *Med. Phys.*, 2013.